PIC/MCC Simulation Computational Modeling of a Ion Thruster Discharge Chamber

IEPC-2013-162

Presented at the 33rd International Electric Propulsion Conference,
The George Washington University • Washington, D.C. • USA
October 6 – 10, 2013

Chen Juanjuan[1], Zhang Tianping[2], Liu Mingzheng[3], Jia Yanhui[4]
Lanzhou Institute of Physics, Lanzhou 73000, China

Abstract: In order to better understand the plasma physical mechanism and real important aspect of discharge plasma processes in the ion thruster discharge chamber thoroughly, a muli-component 2-D computational discharge chamber model is developed. Based on the geometric and physical parameters designated, we could obtain the generational process and the distribution of the plasma by using the PIC simulation to trace the trajectory of particles in the discharge chamber and applying the MCC simulation to studying the collision between the particles. The PIC/MCC model developed in this work tracks following particles: neutrals, singly charged ions, doubly charged ions, secondary electrons and primary electrons.

I. Introduction

Ion thruster, which features the highest efficiency and very high specific impulse compared to other thruster types, propels the spacecraft by accelerating mass and ejecting it from the vehicle. The ejected mass from electric thrusters, however, is primarily in the form of energetic charged particles. With literally hundreds of electric thrusters now operating in orbit on communications satellites, and ion and Hall thrusters both having been successfully used for primary propulsion in deep-space scientific mission[1~3], the future for electric propulsion has arrived. Being one of basic components, discharge chamber utilize direct current electron discharges, radio frequency discharges and microwave discharges to produce the plasma. For improving the performance of the ion thruster discharge chamber, two approaches has been proposed by far. One of these is the experimental testing, another is the analytical method. In addition to the time restriction the experimental technique for extending the performance of ion engines there are other limitations to experimental development work. Experimentally based ion engine research is constricted by its exorbitant cost, the difficulty in performing extensive and detailed parametric studies, and limitations of using the Langmuir probes to access and measure different plasma characteristics for all regions within the discharge chamber. Currently, the design and optimization of present-day

1. Engineer, Lanzhou Institute of physics, chenjjgontp@126.com
2. Professor, Lanzhou Institute of physics,ztp510@aliyun.com
3. Engineer, Lanzhou Institute of physics,liumzh@163.com
4. Engineer, Lanzhou Institute of physics, jiayh510@163.com

ion thrusters is almost entirely based on empirical investigation. Existing theoretical discharge models are useful but do not explain the non-uniform characteristics that are imperative for thruster performance optimization and long-life validation. Compared to the theoretical model[4~6], computational modeling[7~11] can help researchers and designers understand the plasma characteristics, non-uniform plasma densities and non-uniform neutral atom temperatures and densities, and the trajectory and distribution of the plasma. The results can provide reference and reference value in the future development of performance analysis of ion thruster discharge chamber.

The rating values of thruster, specific impulse and efficiency for LIPS-200 ion thruster, which is developed by Lanzhou institute of physics, are 40mN, 3000s, 60% respectively. On the basis oc the experimental data, we have analyzed the performance of the LIPS-200 ion thruster and obtained the geometric and operating parameters. The objective of this investigation is to create a two-D electron bombardment ion thruster discharge chamber model to accurately predict the plasma behavior within the thruster. By using the PIC simulation to trace the trajectory of particles in the discharge chamber and applying the MCC simulation to studying the collision between the particles, we could obtain the generation process of plasma, the number density results for four different particles at the steady condition, and the distribution of the electric-magnetic field.

II. Establish of the Computational Model

Because of symmetric characteristics of LIPS-200 ion thruster discharge chamber, this paper chooses half of it to simulate. The computational domain includes the cathode exit, the cathode keeper walls, the chamber walls, and the screen grid. The magnets are located on the outside surface of the discharge chamber walls. A schematic of the computational domain considered in this work is given in Figure 1.

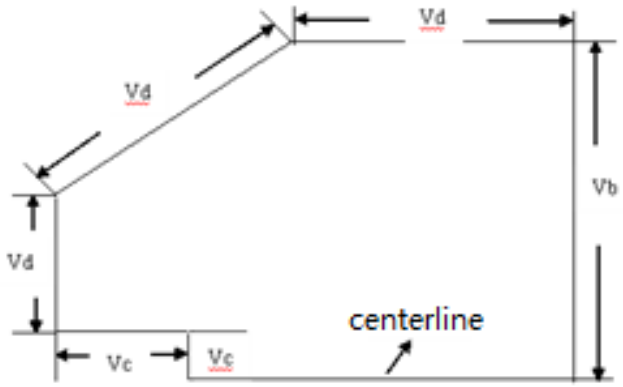

Fig.1 A schematic of the discharge chamber computational domain

For a ion thruster discharge chamber, there are four types of surfaces and five different particles that need to be modeled in terms of particle boundary conditions. These are: cathode potential surfaces, anode potential surfaces, grids and the symmetry boundary line. The particles are: primary electron, secondary electron, xenon ion, double xenon ion and neutral. The electrons that emitted from the cathode or generated by the collision between the different particles hit an anode biased wall they are physically absorbed into the wall, be reflected at the cathode and screen grid potential boundaries, and be reflected with diffuse reflections. At the cathode, anode and the symmetry boundary condition along the centerline of the discharge chamber, the neutral

particles are handled with reflections. Both ions and neutrals have a transparency specified at the screen grid. This transparency determines the faction of particles that make it through the holes in the grid wall to the outside of the discharge chamber. The random number generated by the computer is about 0~1. By comparing this random number and the transparency, we can gain the number of particle that escapes from the discharge chamber. If the value that the random number subtracted from the transparency was negative, the xenon ion would leave the discharge chamber through the grid holes forming the ion beam. On the contrary, xenon ions are absorbed by the screen grid.

Assumptions in this model are as follows:

(1) Because of the minim ratio of the multi-charged xenon ion, this paper neglects the effect of it on the distribution of the electric-magnetic field.
(2) This paper assumes that primary electrons whose energy is about 2eV are created from a hollow cathode. The length of the hollow cathode orifice that electrons exit is about 1mm.
(3) The flow path of primary electrons that leave arbitrarily the cathode source is taken as a stream directed towards the screen grid with a 15 degree half angle divergence.
(4) The discharge loss of the elastically collision between ion and neutral is not calculated.
(5) This paper ignores the magnetic vector potential that generated by the following plasma. The reason is that the value two potential that just do not compare.

III. Simulation Approach and Flowchart

PIC/MCC simulation approach is used to model the LIPS-200 ion thruster discharge chamber. The parameters we adopted are the same with the literature[12]. In a PIC/MCC simulation all plasma particles are tracked using a macro particle assumption along with solving the electric fields based on the charge particle distributions. The large computational requirements for the PIC simulations mainly arise from the need to satisfy numerical parameters such as the grid spacing and the time step size, and to satisfy the stringent stability conditions posed by the basic plasma characteristics. For tracing ion and electron simultaneously, this paper supposes that the ration of the step size between the ion and electron is 50. Once the emission current and time step size of electron is determined, we could obtain the number of electrons that enter the discharge chamber.

A. Static Magnetic Field

Magnetic field produced by the permanent magnets inside the discharge chamber is modeled using a subset of Maxwell's equations. The expression of the magnetic vector potential in cylindrical coordinates gives

$$\frac{\partial}{\partial r}\left(\frac{1}{r\mu}\frac{\partial(rA_\theta)}{\partial r}\right)+\frac{\partial}{\partial z}\left(\frac{1}{\mu}\frac{\partial A_\theta}{\partial z}\right)=\frac{\partial H_{cr}}{\partial z}-\frac{\partial H_{cz}}{\partial r} \tag{1}$$

where μ is the permeability of free space tensor. A_θ is the magnetic vector potential in θ-directon. H_c is the coercive force of the magnets. The boundary conditions required for solving equation (1) are:

$$\begin{aligned} &A_\theta \to 0, r \to \infty; \qquad A_\theta \to 0, z \to \infty \\ &A_\theta \to 0, z \to -\infty; \qquad \frac{\partial A_\theta}{\partial r}=0, r=\infty \end{aligned} \tag{2}$$

The axial and radial components of magnetic field vector are related to the magnetic vector

potential with

$$B_r = -\frac{\partial A_\theta}{\partial z}$$
$$B_z = -\frac{1}{r}\frac{\partial (rA_\theta)}{\partial r} \tag{3}$$

B. Electric Field

The expression of Poisson's equation can be written as

$$\frac{\partial^2 \phi}{\partial r^2} + \frac{1}{r}\frac{\partial \phi}{\partial r} + \frac{\partial^2 \phi}{\partial z^2} = -\frac{e}{\varepsilon_0}(n_i - n_e) \tag{4}$$

where n is the net number density. When the left side of equation (4) is equal to 0, the potential calculated is static electric potential.

Electrons extracted from the hollow cathode enter the discharge chamber and ionize the propellant gas. As expected, the particle originates at the hollow cathode orifice and is magnetically confines at the cusps, reflected from cathode potential surfaces, scattered by elastic collisions, and lost to an anode surface. When the static and dynamic vector potential is determined, the electric potentials are obtained by adding dynamic electric potential values to the static electric potential values by using the principle of superposition. In a particle-particle collision, generally the slow moving heavy particle is treated as the target particle and the fast moving electron is taken as the incident particle. While the energy of electron is greater than 12.13eV, in electron-neutral collisions, a neutral is divided into a electron and a xenon ion. Once the electron energy exceeds 21.1eV, the singly ionized species that collides with electron would be ionized again.

C. MCC Simulation

For ion thruster, it is impossible to trace the trajectory of every particle in discharge chamber. The reason is that the performance and operational speed of an ordinary computer is not sufficient for simulation. This paper applies the mean freedom to the degree of the collision frequency between particles. Herein, we only consider the electron-neutral elastic, excitation and ionization collision, xenon ion-neutral elastic and charge-exchange collision.

The probability for electron-neutral interaction is given by

$$P = 1 - \exp(-n_0 v_e \sigma(\varepsilon_e)\Delta t) \tag{5}$$

where n_0 is the number density of neutral. v_e is the velocity of electron. $\sigma(\varepsilon_e)$ is the electron-neutral collision cross section. Δt is the time step.

If the ration of the random number and the probability of the electron-neutral was less than 1, it expresses that the collision between particles happens. For an elastic collision, there are no new charged particle produced and no energy loss.

Figure 2 shows a flow chart of the computing sequence used by the PIC/MCC simulation utilized in this work.

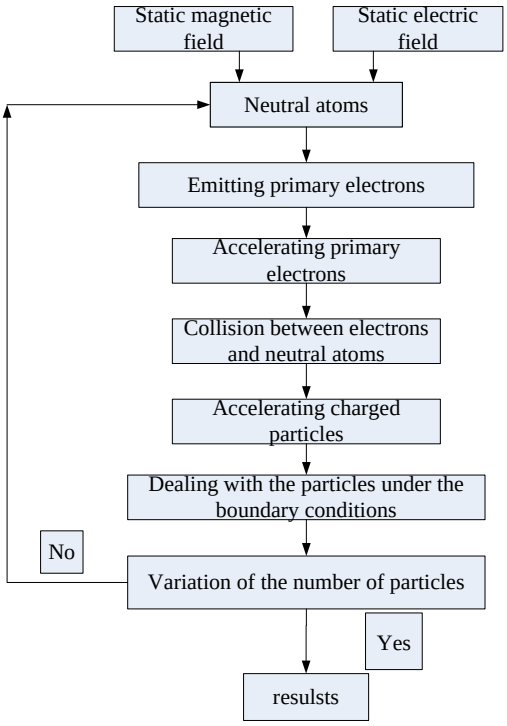

Fig.2 A flow chart of PIC/MCC model showing the computing sequence of LIPS-200 ion thruster discharge chamber

IV. Simulation Results

Figure 3 shows the static magnetic field vector potential contour lines.

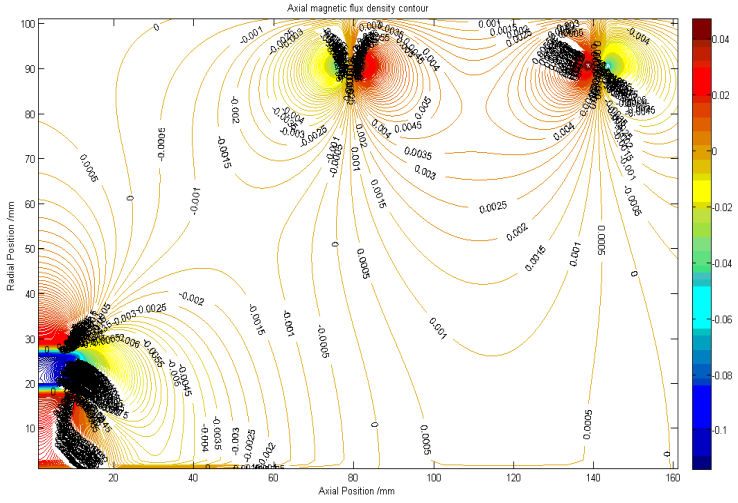

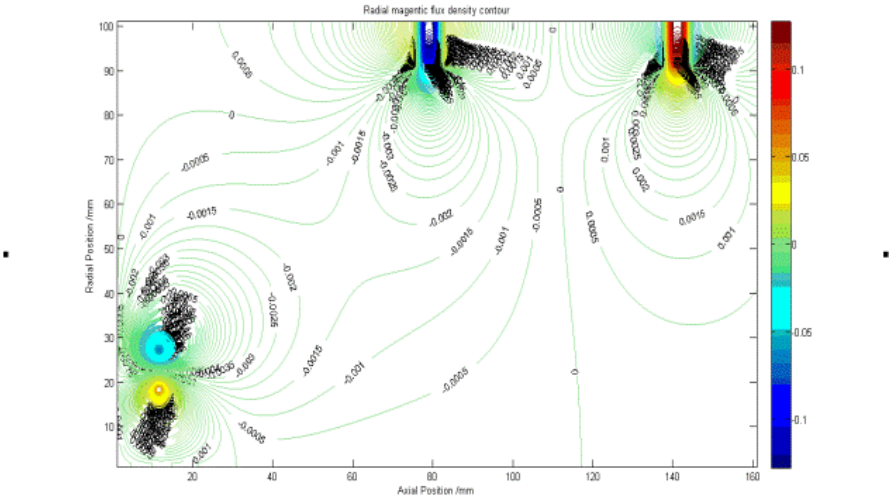

Fig.3 Static magnetic field contours

Figure 3 shows that the magnetic vector potential lines run between the cusp regions of the magnets. The maximum magnetic flux density that is at surface of the magnets is about 1200Gs. From anode wall to the inside of the discharge chamber, the magnetic flux density becomes smaller. The hollow cathode orifice where the value of the magnetic density is about 45Gs, at the same time, larmor radius of electron is 6.87×10-5m. The minimum value is about 5Gs, which is obtained in the symmetric area.

Figure 4 is the static and dynamic electric potential contours in volts at steady state.

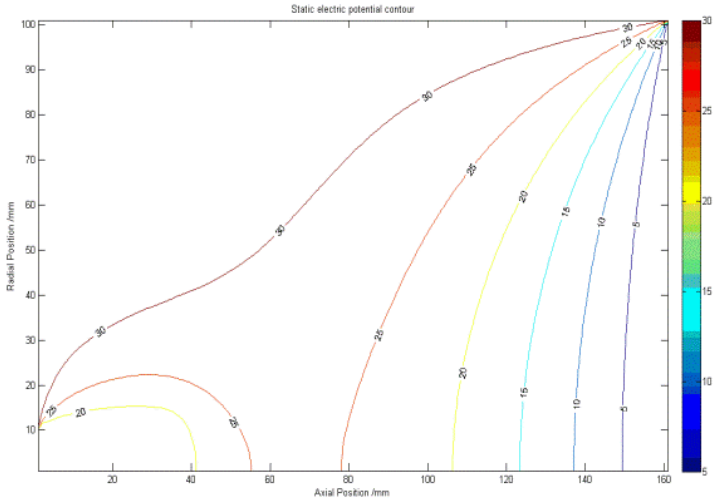

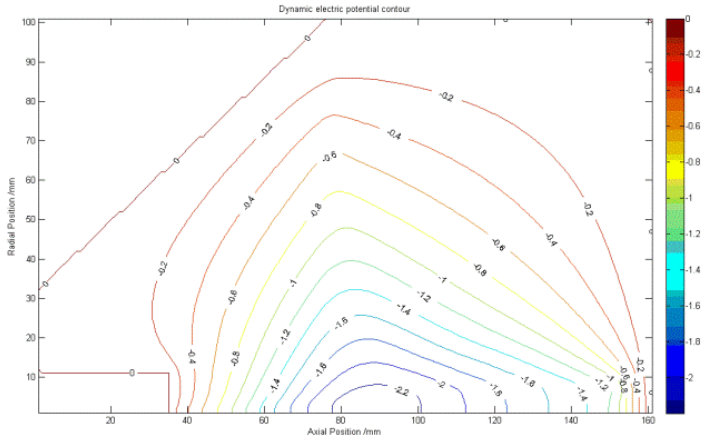

Fig.4 Input static and dynamic electric potential contours in volts

Figure 4 shows that compared to the static electric potential, the dynamic electric potential is greatly small. The value of it is about 0~2.0V, which accords with the experimental results[13]. Consequently, the dynamic electric field would not affect the transportation of charged particles.

Figure 5 shows the axial and radial electric field distribution at steady state.

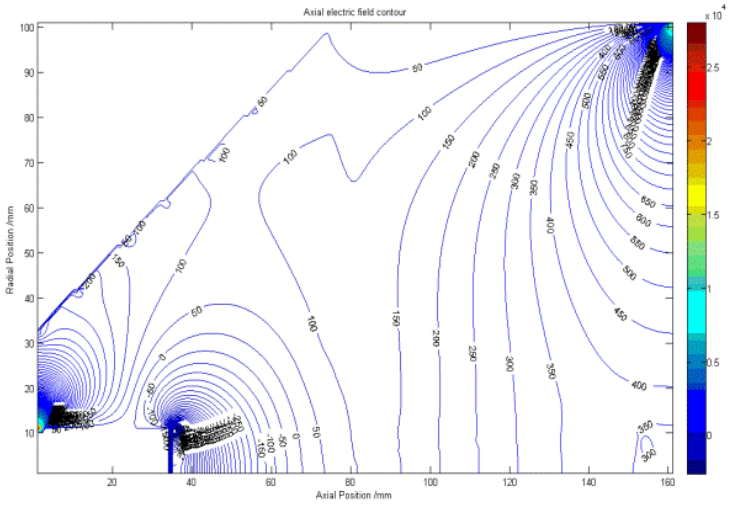

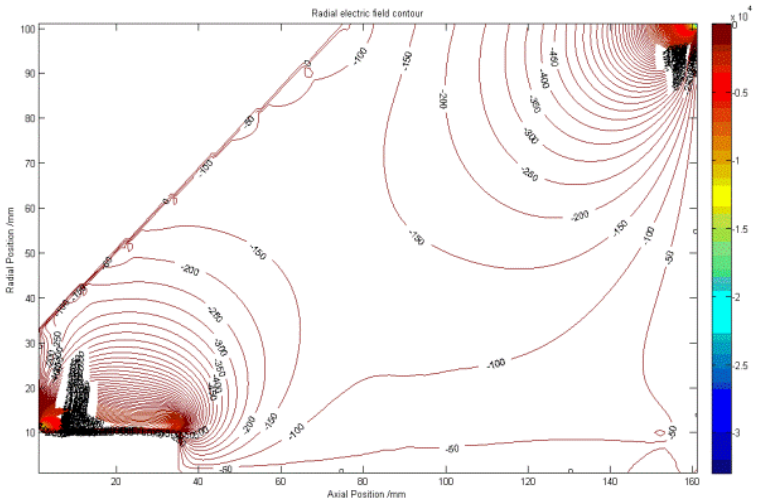

Fig.5 Axial and radial electric field contour

The results show that because the discharge voltage is larger than cathode and screen grid voltage, the electric field of the interface of two walls is so great that it would interact with the charged particles. Along with the positive of axial direction, the electric field would be from the maximum to zero, subsequently, it will be increased gradually. Along with the radial position increasing, the electric field will decrease.

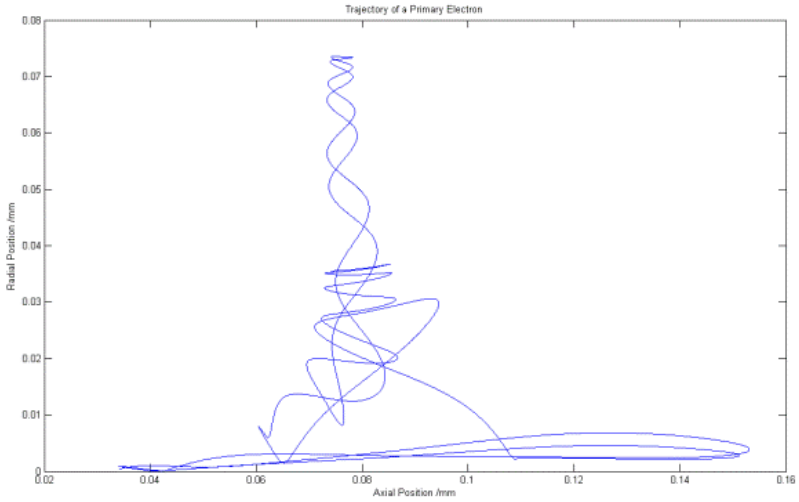

Fig.6 The trajectory of a primary electron

Simulation results show that the primary electron originates at the hollow cathode orifice and is magnetically confined at the cusps. The magnetized electrons then influence the ion motion of the boundaries by electrostatic effects. This causes the ion loss to the cusps to be the Bohm current to the hybrid area.

V. Conclusion

Discharge chamber, as one of the critical component for ion thruster, of which performance is

extraordinarily vital to improve the performance of ion thruster. Compared to the other approaches, computational modeling can help us to better understand the plasma characteristics and the results can be used to improve the performance of the ion thruster. In the future this computational model can be used to improve the design of the next-generation of ion engines and enhance experimental research currently being undertaken. Therefore, on the basis of the experimental and theoretical results, this paper uses the PIC/MCC simulation method to establish the 2-D mathematical model to model the plasma movement in the LIPS-200 ion thruster discharge chamber.

Simulation results show that the primaries are well confined by the strong axial magnetic field component in the LIPS-200 ion thruster discharge chamber, and collisional effects eventually scatter the primary into the cusp loss one. The magnetic vector is maximum at the surface of the magnets. Therefore, from the discharge chamber wall to the inside of the discharge chamber, the magnetic field becomes smaller, the area of symmetry boundary line where the magnetic field is close to zero. The dynamic electric vector potential produced by the movement of the charged particles is so small that it does not affect the transportation of plasma.

Acknowledgments

The authors would like to acknowledge the professor Zhang Tianping for his supported and approach.

References

[1] Tianping Z., "Recent international progress in ion and Hall electric propulsions," Vacuum and Cryogenics, 2006, 12(4): 187~193.

[2] Polk J E, Anderson J R, et al. "The effect of engine wear on performance in the NSTAR 8000 hour ion engine endurance test," AIAA-97-3387,1997.

[3] Kuninaka H, Nishiyama K, Funakai I, Tetsuya K, Shimizu Y and Kawaguchi J. "Asteroid rendezvous of hayabusa explorer using microwave discharge ion engine," IEPC-2005-010,2005.

[4] Brophy J R. "Ion thruster performance model," NASA CR-174810,1984.

[5] Goebel D M, Wirz R E, Katz I. "Analytical ion thruster discharge performance model," AIAA 2006-4486.

[6] Goebel D M, Polk J, Sengupta A. " Discharge chamber performance of the NEXIS ion thruster," AIAA 2004-3813.

[7] Wirz R, Katz I. " 2-D Discharge chamber model for ion thrusters," AIAA 2004-4107.

[8] Wirz R, Katz I. "Plasma processes of DC ion thruster discharge chamber," AIAA 2005-3690.

[9] Wirz R, Goebel D M. "Ion thruster discharge performance magnetic field geometry," AIAA 2006-4487.

[10] Brophy J R, Katz I, Polk J, Anderson J. "Numerical simulations of ion thruster accelerator grid erosion," AIAA 2002-4261.

[11] Wusheng H, Anbang Sun, et al. " Numerical simulation of ion thruster discharge chamber," High power laser and particle beams. 22(12): 3020~2034.

[12] Juanjuan C, Tianping Z, et al. " Performance optimization of 20 cm xenon ion thruster discharge chamber," 24(10): 2469~2473.

[13] Herman D A, Gallimore A D. "Discharge chamber plasma structure of a 30 cm NSTAR-type ion engine," AIAA 2004-3794,2004.